HHS Public Access

Author manuscript

Eur J Pharm Sci. Author manuscript; available in PMC 2024 March 26.

Published in final edited form as:

Eur J Pharm Sci. 2020 December 01; 155: 105560. doi:10.1016/j.ejps.2020.105560.

Laser-assisted skin delivery of immunocontraceptive rabies nanoparticulate vaccine in poloxamer gel

Amit Bansal[a], **Wael Gamal**[a], **Ipshita Jayaprakash Menon**[a], **Victoria Olson**[b], **Xianfu Wu**[b], **Martin J. D'Souza**[a]

[a]Center for Drug Delivery Research, Vaccine Nanotechnology Laboratory, Mercer University, College of Pharmacy, Atlanta, GA, 30341 USA

[b]Poxvirus and Rabies Branch, DHCPP, NCEZID, Centers for Disease Control and Prevention, Atlanta, GA, 30329 USA

Abstract

A painless skin delivery of vaccine for disease prevention is of great advantage in improving compliance in patients. To test this idea as a proof of concept, we utilized a pDNA vaccine construct, pDNAg333-2GnRH that has a dual function of controlling rabies and inducing immunocontraception in animals. The pDNA was administered to mice in a nanoparticulate form delivered through the skin using the P.L.E.A.S.E.® (Precise Laser Epidermal System) microporation laser device. Laser application was well tolerated, and mild skin reaction was healed completely in 8 days. We demonstrated the adjuvanted nanoparticulate pDNA vaccine significantly upregulated the expression of co-stimulatory molecules in dendritic cells. After topical administration of the adjuvanted nano-vaccine in mice, the high avidity serum for GnRH antibodies were induced and maintained up to 9 weeks. The induced immune response was of a mixed Th1/Th2 profile as measured by IgG subclasses (IgG2a and IgG1) and cytokine levels (IFN-γ and IL-4). By flow cytometry, we revealed an increase of $CD8^+$ T-cells and CD45R B-cells upon the administration of the adjuvanted vaccine. By comparison to our previous study using the same pDNA nanoparticulate vaccine through an IM route, a comparable immune response was induced using P.L.E.A.S.E. However, the vaccine dose in the current study was four-fold less than what was applied through the IM route. We concluded that laser-assisted skin vaccination has a potential of becoming a safe and reliable vaccination tool for rabies vaccination in animals or even in humans for pre- or postexposure prophylaxis.

Keywords

Laser microporation; Skin vaccination; Particulate vaccine; Adjuvant; Rabies vaccines

Correspondence: Amit Bansal, 3001 Mercer University Drive, DV-108, Atlanta, GA 30341, Fax 678 547 6364, amit.bansal@live.mercer.edu, **Present Address:** 655 Hooker Road, Allegan, MI 49010.

Disclosure

The authors report no conflicts of interest in this work. The authors alone are responsible for the content and writing of this article.

1. INTRODUCTION

Rabies as an ancient disease has evolved since the time of Pasteur to obtaining a neglected disease status today, but it still causes around 65,000 human deaths annually in the world, with >95% of these in Asia and Africa [1,2]. Among the reasons why this vaccine-preventable disease is still such a burden in endemic regions include a lack of political will, disease ignorance and limited resources, in addition to the complicated vaccination regimen in human postexposure prophylaxis (PEP). There is a continued need for novel vaccines, formulations, and delivery methods to simplify PEP. Rabies is a typical zoonosis and has a broad range of animal hosts, including terrestrial mammals and bats. Frequent or occasional rabies transmission from animals to humans makes elimination of the disease extremely challenging, if not impossible. The dual control of rabies and animal populations is one idea we are actively exploring [3]. The pDNAg333-2GnRH vaccine has a unique dual function of rabies control and immunocontraception in animals. This construct has a sterility-inducing potential through production of antibodies against gonadotropin-releasing hormone (GnRH, a master reproductive growth hormone). Blocking the binding of GnRH to its receptors in the pituitary gland prevents the production of luteinizing hormone (LH) and follicle stimulating hormone (FSH) which are essential for reproductive functions, leading to sterility in animals [4,5]. Duplication of the GnRH in the pDNA was constructed to offset the weak immunogenicity in the vaccine [6–8]. It is always desirable to develop a single dose vaccine due to the difficulty and inconvenience that decreases compliance with multi-dose administration [9]. Our previous studies demonstrated that particularization of vaccine imparted more immunogenicity, required no booster dose, and provided additional benefits for vaccine storage at room temperature [7,8]. The objective of this study was to investigate the efficacy of the pDNA vaccine in a nanoparticulate form via skin delivery.

The delivery of antigen via skin has gained interest in the recent years due to its specialized immunological network. Different layers of the skin are rich in immunocompetent cells, such as Langerhans cells (LCs) and dermal dendritic cells (DCs) [10,11]. These antigen-presenting cells recognize, uptake, and present foreign antigens to T and B cells in the draining lymph nodes to initiate adaptive immune responses. Skin vaccination can reduce the dose up to one-fifth of the conventional dose and generate immune responses comparable to intramuscular (IM) and subcutaneous (SC) vaccination [12]. Skin vaccination has shown significant efficacy in controlling various infectious diseases, such as smallpox and tuberculosis [13]. A major challenge to deliver antigens into the epidermis and dermis layers of the skin is the skin's outer barrier, stratum corneum, that has a significant resistance to the delivery of hydrophilic drugs and vaccine antigens [14,15]. In the current study, we delivered the pDNA vaccine topically using a laser-based device that can create aqueous micropores in the skin through controlled ablation of the skin layers, thus bypassing the stratum corneum. Precise Laser Epidermal System (P.L.E.A.S.E, Pantec Biosolutions) used in the current study employed an Er: YAG laser that has the advantage of enabling cold ablation and producing little or no microthermal zones in the vicinity of the application site. The Er: YAG laser emits energy at 2940 nm, mimicking the absorption peak of water, and when contacts the skin, leads to the formation of aqueous pores. Early version Er: YAG laser devices either generate a single laser beam or use a grid to split the beam and

fractionate the energy to create multiple micropores. The device utilizing grid requires manual adjustment and may produce non-homogenous pores. However, the modified P.L.E.A.S.E device used in this study utilizes a scanner (beam deflection unit) that adjusts the laser in a predefined pattern to fractionate the energy. This device can produce hundreds of pores using pre-programmed settings in a few seconds. The laser beam generates pores of controlled dimensions and depths using laser fluence (energy per unit area) without affecting surrounding tissues and reducing the risk of inhomogeneity [16,17].

Using the P.L.E.A.S.E device in mice to deliver a pDNA nanoparticulate vaccine dispersed in the poloxamer gels, we found laser-assisted skin vaccination has the potential to become a safe and reliable vaccination tool for rabies vaccination in animals or even in humans for prophylaxis.

2. MATERIALS AND METHODS

Cell culture materials RPMI 1640 medium, Dulbecco's Modified Eagle medium, fetal bovine serum (FBS), penicillin/streptomycin, sodium pyruvate and nonessential amino acids were obtained from Cellgro Mediatech (Herndon, VA, USA). Mouse dendritic cells (DC2.4) were given as a kind gift from Dr. Kenneth L. Rock (Dana-Farber Cancer Institute, Inc., Boston, MA, USA). Six- to eight-week-old Swiss Webster female mice were purchased from Charles River Laboratories (Wilmington, MA, USA). GnRH peptide conjugated to bovine serum albumin (BSA) was bought from New England Peptide, Inc. (Gardner, MA, USA). Antibodies used to stain cells for MHC I, MHC II, IFN-γ, IL-4, CD45R, CD62L, CD4 and CD8 for flow cytometry analysis were purchased from eBioscience laboratories (San Diego, CA, USA). HRP-tagged secondary goat anti-mouse IgG was procured from Invitrogen (Rockford, IL, USA). BSA, polyvinyl alcohol, dichloromethane, and PLGA (Mw 7,000-17,000) were purchased from Sigma (St Louis, MO, USA). Chitosan glutamate (Sea Cure (+) 210) was purchased from Protan, Inc. (Portsmouth, NH, USA).

2.1 Fabrication of PLGA-chitosan nanoparticles and loading of pDNA

Nanoparticles were prepared by the emulsification method described in detail in our previous publications [7]. Briefly, a suitable amount of PLGA (Mw 7,000-17,000, Sigma, St Louis, MO, USA) was added to dichloromethane (DCM) (Sigma, St Louis, MO, USA), which comprised the organic phase. The aqueous phase consists of polyvinyl alcohol (PVA) (Sigma, St Louis, MO, USA) in water (Millipore, Billerica, MA, USA) and was then added to the organic phase under homogenization. The formulated w /o emulsion was later added to the second aqueous phase containing PVA and chitosan glutamate (Sea Cure (+) 210, Protan, Inc., Portsmouth, NH, USA) under homogenization to form a w/o/w multiple emulsion. The nanoparticle suspension was further washed with deionized water and freeze-dried using trehalose as a cryoprotectant [18,19].

Loading of pDNA on nanoparticles was achieved by incubating pDNA with the nanoparticle suspension for 30 minutes. After incubation, samples were centrifuged and supernatants were collected and analyzed for pDNA concentration using the Nanodrop 2000C spectrophotometer (Thermo Scientific, DE, USA). Mass balance approach was used to

calculate the amount of pDNA adsorbed on the nanoparticles by subtracting the amount of pDNA in the supernatant from the initial amount of pDNA [20–22].

2.2 Immunization of mice

Swiss Webster mice were used to study the antigenicity of the pDNA nanoparticulate vaccine. The mice were housed under specific pathogen-free conditions in accordance with the approved Institutional Animal Care and Use Committees (IACUC) protocol at Mercer University. Mice were divided into three groups; the first group (n=6) received pDNA in hydrogel (negative control), the second group (n=6) received pDNA nanoparticulate vaccine in hydrogel and the third group (n=6) received pDNA nanoparticulate vaccine with adjuvants (Alum and MF59) in hydrogel. Before immunization, micropores were created on the prepared dorsal skin surface of the mice using the P.L.E.A.S.E.® device. The nanoparticulate vaccine was dispersed in a poloxamer hydrogel and was applied onto the skin micropores. Mice were dosed with one prime dose (25 μg of pDNA) on day 0. Sera was collected weekly until the end of study on week 9 to measure specific antibody levels against GnRH.

2.3 Laser microporation on the mouse skin

The dorsal surface of the mice was prepared for microporation by removing the hair using clippers. The micropores were created on the mouse skin using the P.L.E.A.S.E.® professional fractional infrared laser system (Pantec Biosolutions, Ruggell, Liechtenstein). The laser microporation was performed at 200 Hz, at 125 μs pulse duration, with a fluence of 17.8 J/cm^2 with 2 pulses per pore. The pore array size was 8 mm and a pore density of 6.5% was used. Approximately 80 pores were created with an average pore diameter of 220 μm.

2.4 Scanning electron microscopy

Scanning electron microscopy (SEM) was carried out to evaluate morphology of pores formed on the surface of laser-treated skin of the mice. Metal stubs were used to mount the skin using double-sided carbon conductive tabs. Mounted skin samples were then imaged at various magnifications. Images were captured from the dorsal side (stratum corneum side) and ventral side (dermis side) of skin and were examined using the Phenome benchtop SEM, Nanoscience Instruments, Phoenix, AZ [23].

2.5 Quantification of antigen maturation markers, CD40 and CD80 expression

Before testing the *in-vivo* efficacy of the pDNA nanoparticulate vaccine in mice, we evaluated the *in-vitro* performance of the vaccine using DC2.4 cells for the expression of maturation markers. Dendritic cells (DC2.4) were plated at 5 × 10^4 cells per well in a 48-well plate and incubated at 37 °C for 24 h. Then the adherent DC2.4 cells in each well were pulsed using 50 μg of vaccine nanoparticles (equal to 1 μg of pDNA) along with adjuvant particles and further incubated at 37 °C for 24 h. After completion of incubation, the cells were washed with Hanks balanced salt solution (HBSS) to remove extracellular nanoparticles for harvesting. The cells were harvested using the cell scraper and collected in eppendorf tubes. The cells were centrifuged at 350 × g for 5 min, and resuspended

for staining using fluorescein isothiocyanate (FITC) labeled antimouse CD40 and CD80 maturation markers at a dilution of 1:50 (eBioscience laboratories, San Diego, CA). After incubation at 4 °C for 1 h, the stained cells were washed twice using HBSS, and the measurement of maturation markers was performed on the BD Accuri C6 flow cytometer (BD Bioscience, San Jose, CA).

2.6 Detection of Anti-GnRH antibodies by ELISA

GnRH antibodies (IgG, IgM, IgG1, and IgG2a) were analyzed using the enzyme-linked immunosorbent assay (ELISA). Briefly, the flat bottom poly-L-lysine coated high binding 96-well plate was coated with 1 μg (100 μL/well) of GnRH peptide conjugated to BSA (GnRH-BSA) at 4 °C overnight. The wells were blocked with 5% (w/v) BSA in phosphate buffered saline (PBS, 0.01M, pH 7.2) at room temperature (RT) for 2 h. The immunized mouse serum samples were then added to the wells at 1:100 dilution in PBS containing 5% (w/v) BSA, and incubated at RT for 2 h. After 3 washes of the plate with PBS containing 0.05% Tween-20 (PBST), the HRP-tagged secondary goat anti-mouse IgG, IgG1, or IgG2a at 1:2,000 dilution in PBS containing 5% (w/v) BSA was added to each well and incubated at RT for 1 h. The substrate 3,3′,5,5″-tetramethyl-benzidine (TMB) at 2.08 mM was used to develop color and the reaction was stopped using 2M sulfuric acid. The optical density was measured at 450nm using a microplate reader (BioTek instruments Inc., Winooski, VT, USA) [24]. The assays were performed in triplicate and the results expressed as mean ± SEM.

2.7 Avidity assay by elution ELISA

An avidity index (AI) is defined as the concentration of sodium thiocyanate (NaSCN) that results in a 50% reduction in absorbance from untreated wells. The avidity (AI) of anti-GnRH antibodies was determined by NaSCN elution ELISA assay. An AI of 1 correlates to high avidity, whereas an AI close to 0 correlates to low avidity. The procedure for avidity measurement was similar to the IgG subclass ELISA, with an additional step in which 50 μL of NaSCN (a chaotropic compound that interferes with antigen-antibody reaction) at 0.1-0.8M was added to the well after completion of Ag-Ab reactions. The plate was further incubated at RT for 20 min, and the AI was measured by absorbance at 450 nm using a microplate reader (BioTek instruments Inc., Winooski, VT, USA) [25,26].

2.8 Measurement of T cells, B cells, and memory immune response in the lymphatic organs

After completion of immunization mice were euthanized, the spleen and lymph nodes were collected for single cell suspension preparation using the 40-μm cell strainer. The viability of cells was checked by trypan blue exclusion method using an automated cell counter (Bio-Rad, Hercules, CA). Viable cells at the concentration of 1×10^6 cells/mL were collected in a 1.7 mL Eppendorf centrifuge tube for detecting the T or B cell markers. For T cell analysis, the anti-mouse CD8 FITC, CD62L APC markers were added to the lymphocytes. For B cell analysis, mouse antibodies against CD45R FITC and CD27 APC were added to the lymphocytes. The reactions were kept in the dark and incubated for 1 h on ice. After incubation, the cells were centrifuged and washed twice using PBS (0.01M, pH 7.2), and

were resuspended in 200 μL PBS. The cells were analyzed using the flow cytometer, BD Accuri™ C6 Plus (BD Accuri Cytometers, Ann Arbor, MI) [27,28].

2.9 Intracellular Staining

The intracellular staining allows simultaneous analysis of cell surface markers by combining fixation and permeabilization in a single step. Immune cells were harvested from mouse spleen, and single cell suspension was prepared by using a 40-μm cell strainer. The cells were first cultured for 3 h in complete DMEM supplemented with 2-mercaptoethanol at 50 μM, followed by incubation for 1 h in the presence of brefeldin at 1μg/mL. After washing, the cells were incubated with $CD4^+$ T cell-FITC for 1 h. The cells were then centrifuged at 350 × g for 5 min, washed twice in PBS (0.01M, pH 7.2), and resuspended in Foxp3 fixation/permeabilization solution for incubation at 4 °C for 30 min in the dark. Subsequently, the cells were centrifuged and the cell pellet was suspended in permeabilization buffer at RT with IL-4, IFN-γ APC cytokine markers for 30 min in the dark. Cells were further washed in permeabilization buffer and finally suspended in PBS for analysis using the flow cytometry [29,30].

2.10 Statistical Analysis

All experiments were performed in triplicate, unless otherwise indicated. Data analyses were performed using Graphpad Prism version 5 and expressed as mean values ± SEM. One-way ANOVA and post-hoc Tukey test was used for multiple comparisons. A p value < 0.05 was considered significant, < 0.01 very significant, and < 0.001 extremely significant.

3. RESULTS

3.1 Physical characterization of rabies pDNA nanoparticulate vaccine

Nanoparticles were prepared using the emulsification method. Their size ranged from 350-450 nm and the zeta potential was 50.0 ± 5.0 mV. The polydispersity index (PDI) of the nanoparticulate vaccine formulation was < 0.7, indicating particles having a narrow size distribution. The pDNA alone is negatively charged and adsorbed on the surface of positively-charged nanoparticles due to electrostatic attraction. The pDNA to nanoparticles ratio (P/N) of 1/50 was used for the study, as it resulted in complete adsorption of pDNA and showed in our previous publication [7].

3.2 Scanning Electron Microscopy

SEM images for skin samples exposed to laser radiation were captured at different magnifications in order to visualize the morphology of skin and pores. Figure 1A was a control skin sample (310×) that had not been exposed to radiation. Figure 1B showed the pores on laser-treated skin at 195× magnification, and Figure 1C presented a single pore at a higher magnification of 500. We also took the images of the dermis side of laser-treated skin at 500× and found no pores, indicating these pores created from the top did not pierce the dermis side of the skin (Figure 1D).

3.3 Pore Closure Study

In this experiment, we aimed to determine the time required to heal the skin of mice after exposure to laser radiation. During the healing process, skin redness around the pores was observed in the irradiated region. Redness started on day 2 and persisted until day 4, then gradually diminished. Complete recovery of the skin characterized by pore closure was seen on day 8 (Figure 2).

3.4 The expression of CD40 & CD80 in DC2.4 was increased using the adjuvanted pDNA nanoparticulate vaccine

The ability of nanoparticulate vaccine to deliver pDNA and upregulate costimulatory markers (i.e., CD40 and CD80) on DC2.4 surface was tested *in vitro*. Maturation of DC2.4 cells is correlated to upregulation of costimulatory molecules which is essential for the T cell activation and proliferation [31]. DC2.4 cells were pulsed with pDNA Vac, pDNA NP Vac, and pDNA NP Vac+Adj, respectively. In Figure 3, the mean fluorescence intensity (MFI) ratio of test groups to untreated control group was higher in all test groups for both CD40 and CD80 expressions. The results also showed particularization of pDNA vaccine significantly enhanced the MFI for both CD40 ($p < 0.01$) and CD80 ($p < 0.05$) over soluble pDNA vaccine. Addition of adjuvants to pDNA nanoparticulate vaccine further enhanced the expression of both CD40 and CD80 molecules by comparison to the soluble pDNA vaccine (CD40, $p < 0.001$; CD80, $p < 0.01$). Increased MFI of CD80 over CD40 was observed in non-adjuvanted vaccine groups, which might suggest a high potential for the activation and proliferation of naïve $CD8^+$ T cells over $CD4^+$ T cells. The addition of adjuvants potentiates the expression of CD40 relative to CD80, and could be associated with a humoral immune response, and thus resulted in a balanced expression of CD40 and CD80.

3.5 Dynamics of GnRH antibody production was characterized in the immunized mice

Fourteen days after a single dose of vaccine using the P.L.E.A.S.E device, no mice from the 3 groups produced a noticeable anti-GnRH antibody titer. In the pDNA Vac group, the GnRH antibody started rising on week 4, peaked on week 5, and maintained peak level to week 8. In mice vaccinated with pDNA NP Vac with or without adjuvant, the anti-GnRH antibodies started rising on week 3, peaked on week 6, and maintained at a high level until week 8 (Figures 4A and 4B). Anti-GnRH antibodies were higher in both the pDNA NP Vac and pDNA NP Vac+Adj groups than the pDNA vaccine group from week 3 through week 8. The anti-GnRH antibodies in the adjuvanted group were always significantly higher than the non-adjuvanted groups (Weeks 3-4: $p < 0.01$, pDNA Vac; Weeks 5-8: $p < 0.001$, pDNA Vac; $p < 0.05$, pDNA NP Vac). These data illustrated that adjuvanted pDNA NP Vac could induce a stronger anti-GnRH antibody response. We also measured the IgM antibody response, the body's first line of defense against infection, and found the IgM titer was high on week 3 and declined from week 6 through 8 (Figure 4C). The reduction in IgM could be due to the rise of IgG that provides long-term immunity.

3.6 The adjuvanted pDNA nanoparticulate vaccine induced a mixed Th1/Th2 response in mice

Mouse sera collected on week 6 were used to determine the levels of IgG subclasses. Figure 5A and 5B, revealed the particulate vaccine exhibited enhanced absorbance for both IgG2a and IgG1 over the soluble vaccine. Supplementation of pDNA NP Vac with adjuvant further potentiated the immune response. The levels of IgG2a in the adjuvanted pDNA NP Vac group were significantly higher than those in the pDNA Vac ($p < 0.01$) and pDNA NP Vac ($p < 0.05$) groups (Figure 5A). Likewise, the levels of IgG1 in the adjuvanted pDNA NP Vac group was significantly higher than those in the pDNA Vac ($p < 0.001$) and pDNA NP Vac ($p < 0.01$) groups (Figure 5B). The IgG2a/IgG1 ratio >1, suggesting a predominant Th1 cytotoxic response, was detected in the non-adjuvanted vaccine groups. In contrast, we observed an IgG2a/IgG1 ratio <1 in the adjuvanted groups, potentiating a Th2 humoral response. Overall, a balanced and mixed Th1/Th2 response was achieved in the adjuvanted nanoparticulate vaccine groups (Figure 5A and 5B).

3.7 High avidity antibodies were induced by the adjuvanted pDNA nanoparticulate vaccines

High avidity antibodies are capable of responding to low levels of cognate antigen after vaccination [32]. Here we measured the avidity index (AI) of anti-GnRH antibodies after immunization in mice. The serum samples were collected on weeks 3, 6, and 9. The AI values were calculated and compared among treatment groups: pDNA Vac, pDNA NP Vac, and pDNA NP Vac+Adj. In Figures 6A, 6B, and 6C, the AI on week 3 was 0.1M for pDNA Vac, and 0.3M for both pDNA NP Vac and pDNA NP+Adj. The AI values increased in all treatment groups over time after vaccination. The AI values of pDNA NP Vac and pDNA NP Vac+Adj were higher than that in the pDNA Vac group, indicating the role of vaccine particularization and adjuvant in inducing high avidity antibodies.

3.8 T cells, B cells, but not memory B cells were increased after re-stimulation by the adjuvanted pDNA nanoparticulate vaccine

The splenocytes and lymph nodes in mice were harvested for cultivation 9 weeks after completion of immunization and re-stimulated *in-vitro* with the formulated vaccines. In splenocytes, $CD8^+$ T cells were significantly increased in the adjuvanted and non-adjuvanted NP Vac groups compared to the pDNA Vac group: 3.9% to 5.0% for pDNA Vac vs pDNA NP Vac, and 3.9% to 6.5% for pDNA Vac vs pDNA NP+Adj ($p < 0.01$) (Figure 7A). The expression of CD62L in $CD8^+$ T cells did not show any noticeable change. For B cells using the CD45R marker, 71.7% of splenocytes were positive in the pDNA Vac group, 75.5% in the pDNA NP Vac group, and 77.0% in pDNA NP+Adj group (Figure 8A). The change of memory B cells (CD27) was negligible between pDNA Vac and pDNA NP groups, but decreased markedly to 1.0% in the adjuvanted group.

In lymph nodes, $CD8^+$ cells were also enhanced and in particular, in the adjuvanted vaccine groups: 12.3% to 15.1% for pDNA Vac vs pDNA NP Vac, and 12.3% to 16.6% for pDNA Vac vs pDNA NP+Adj ($p < 0.05$) (Figure 7B). The expression of CD62L in $CD8^+$ cells was highest in the pDNA Vac group (5.5%), decreased to 4.7% in the pDNA NP Vac and 4.1% in the pDNA NP+Adj. For B cells, 48.6% of lymph node cells were positive for

CD45R in the pDNA Vac group, 55.6% in the pDNA NP Vac, and 64.8% in the pDNA NP+Adj group ($p < 0.05$) (Figure 8B). However, memory B cells showed a downward trend among the comparisons: 36.2% to 29.1% for pDNA Vac vs pDNA NP Vac, and 36.2% to 20.4% for pDNA Vac vs pDNA NP+Adj group. Overall, we observed an enhanced trend of cytotoxicity and humoral immune response when the vaccine was fabricated in nanoparticles and formulated with adjuvants.

3.9 High expression of IL-4 by the adjuvanted pDNA nanoparticulate vaccine, suggesting a Th2 response

Splenocytes harvested from mice were evaluated for expression of IL-4 and IFN-γ to determine the polarization of Th1 or Th2 after immunization. High level of IFN-γ was detected in pDNA NP Vac ($p < 0.01$) and pDNA NP Vac+Adj ($p < 0.001$) when compared to pDNA Vac group. Addition of adjuvant to the vaccine only marginally increased IFN-γ, suggesting a Th1 immune response when the nanoparticulate vaccines were administrated in mice (Figure 9A). However, the IL-4 was significantly higher in pDNA NP Vac ($p < 0.05$) and pDNA NP Vac+Adj ($p < 0.001$) when compared to pDNA Vac group. The adjuvant boosted the expression of IL-4, leading to a Th2 polarization (Figure 9B).

4. DISCUSSION

The pDNA is a plasmid DNA vaccine platform on which a dual vaccine pDNAg333-2GnRH had been constructed, and previously investigated [7,8]. Rabies vaccines are mostly delivered by IM injections; the SC inoculation is no longer applied to human rabies vaccines but to some animal rabies vaccines, and the ID administration has been recommended for human rabies prophylaxis for the sake of cost- and dose- saving. However, the ID injection is technically difficult to perform, and is often painful to the patient [33]. To simplify and improve vaccinations, here we investigated the newly modified laser-assisted skin delivery technology, P.L.E.A.S.E, for rabies vaccination. The laser energy created an array of micropores on the skin surface to serve as small “vaccine depots” [Figures 1 and 2]. Since these micropores are not deep enough to touch the nerves, the process is painless. The P.L.E.A.S.E is different from the ID regimen in which the micropores cause skin redness (mild inflammation) and could lead to enhanced immune response. This was the first time a rabies plasmid DNA vaccine had been tested using the technology. Our study was intended to determine whether the micropores were sufficient to deliver the pDNA effectively and induce an adequate immune response against GnRH, and if so, what the immune dynamics and profiles could be.

The pDNA in the current study has already been characterized to possess the unique function of not only immunocontraception but also rabies prevention [6–8]. Vaccine adsorbed on particulates confers the benefits of enhanced stability and low dose immunization, since antigens on the nanoparticles are cross presented more efficiently at lower concentration (1000-10000 fold) by antigen presenting cells [34]. The hydrogel was used to retain the pDNA vaccine on the site of application to prevent it from spilling out of the skin. The micropores generated by the P.L.E.A.S.E only penetrate epidermis and dermis, which are rich in LCs and DCs. As confirmed in our study by the SEM images,

the micropores on the epidermis side of the skin did not pierce the dermis side [Figure 1]. Mild skin reaction and some thermal damage to the tissues surrounding the micropores were observed and characterized by redness [Figure 2]. Additionally, we observed skin re-epithelialization took approximately 7-8 days rather than 1-2 days as reported previously in skin healing [17]. The relatively long process for the micropores to close (healing) may have contributed to the immune response in our study.

Before evaluating the efficacy of pDNA nanoparticulate vaccine *in vivo*, we investigated its *in vitro* potential by exposing DC2.4 to the vaccine and measured the co-stimulatory molecules of CD40 and CD80. Upregulation of co-stimulatory molecules on DC2.4 cell surface is critical for activation and proliferation of T cells in order to elicit an adaptive immune response. Upon antigen uptake, DC2.4 cells undergo processing and exporting of the antigenic peptide to the immunological synapse by MHC molecules [35]. Interaction of CD40 to CD40L and CD80 to CD28 lead to activation and proliferation of naïve $CD4^+$ T cells and $CD8^+$ T cells. Results of the *in vitro* studies revealed non-adjuvanted pDNA vaccine induced more expression of CD80, suggesting a bias toward MHC I mediated cytotoxic response after pDNA Vac immunization. However, for both rabies protection and immunocontraception, humoral immune responses are the most important for efficacy. By adding adjuvants to the vaccine, we skewed the immune response toward a Th2 profile by marked increase of MFI of CD40 over CD80 [Figure 3]. As tested in the subsequent mice immunizations, the GnRH antibodies were the highest in the adjuvant group, followed by the nanoparticulate vaccine group, and the soluble form pDNA group being the least [Figure 4A and 4B].

The type of IgG subclass after vaccination affects the quality of immune response. Successful vaccination against endogenous molecules, such as GnRH, requires not only neutralizing antibodies but also opsonization antibodies. Siel *et al.,* reported that IgG2a Th1 biased immune response was not effective alone in immunocastration in mice, unless reinforced by IgG1 antibodies and IL-4 cytokines [36]. Rabies vaccination by ID induced both antibody subclasses of IgG1 (neutralizing) and IgG2a (opsonic). Hessenberger, *et al.,* reported that vaccination via skin disruption favors the Th2 response, including induction of IgG1 and secretion of IL-4 by Th2 cells [37]. Interestingly, here we found a high Th1 profile in the non-adjuvanted pDNA vaccine groups, as demonstrated by high IgG2a and IFN-γ levels. This discrepancy could be due to the inherent property of our vaccine, or that the traditional ID is different from the P.L.E.A.S.E. method in vaccine delivery. Addition of adjuvants to the pDNA boosted the levels of IgG2a and IL-4, and skewed toward a Th2 profile. One challenge for vaccine delivery using the P.L.E.A.S.E device is the small amount of antigens that can be delivered to the micropores in the treated skin. The high AI antibodies after immunization could compensate for this limitation of low antigen delivery. In our study, we found the AI was higher in the adjuvanted group than the non-adjuvanted groups and was maintained up to 9 weeks when the experiment was terminated [Figure 6].

Overall, we achieved comparable immunologic results using the P.L.E.A.S.E device to deliver the pDNA vaccine as was seen by IM delivery [8], but the vaccine was one-fourth the dosage of the IM method.

5. CONCLUSIONS

We demonstrated the proof-of-concept topical administration of a plasmid DNA vaccine using the P.L.E.A.S.E device. The delivery was well tolerated in mouse skin with mild inflammation, which may further boost the antigen immune response. One concern could be the “risk management” after vaccination, with antigen exposed to the skin surface for an extended period before recovery. Our data suggested the laser-assisted skin delivery of pDNAg333-2GnRH nanoparticular vaccine generated both cellular and humoral immune responses, and adding of adjuvant to the vaccine skewed the immunity toward a Th2 profile.

Acknowledgements

The authors would acknowledge the use of facilities of Vaccine Nanotechnology Laboratory, Department of Pharmaceutical Sciences, College of Pharmacy and Health Sciences, Mercer University, Atlanta, GA. The results of the study will be a part of Amit Bansal’s dissertation.

Funding

This research did not receive any specific funding from agencies in the public, commercial, or not-for-profit sectors.

The findings and conclusions in this report are those of the authors and do not necessarily represent the views of the Centers for Disease Control and Prevention.

References

[1]. Wilde H, Ghai S, Hemachudha T, Rabies: Still a silent killer targeting the poor, Vaccine. 35 (2017) 2293–2294. 10.1016/j.vaccine.2017.03.001. [PubMed: 28343778]

[2]. Wilde H, Lumlertdacha B, Meslin FX, Ghai S, Hemachudha T, Worldwide rabies deaths prevention--A focus on the current inadequacies in postexposure prophylaxis of animal bite victims, Vaccine. 34 (2016) 187–189. 10.1016/j.vaccine.2015.11.036. [PubMed: 26626211]

[3]. Wu X, Smith TG, Franka R, Wang M, Carson WC, Rupprecht CE, The feasibility of rabies virus-vectored immunocontraception in a mouse model, Trials Vaccinol. 3 (2014) 11–18. 10.1016/j.trivac.2013.11.003.

[4]. Sharma S, McDonald I, Miller L, Hinds LA, Parenteral administration of GnRH constructs and adjuvants: immune responses and effects on reproductive tissues of male mice, Vaccine. 32 (2014) 5555–5563. 10.1016/j.vaccine.2014.07.075. [PubMed: 25130539]

[5]. Fagerstone KA, Miller LA, Killian G, Yoder CA, Review of issues concerning the use of reproductive inhibitors, with particular emphasis on resolving human-wildlife conflicts in North America, Integr. Zool 5 (2010) 15–30. 10.1111/j.1749-4877.2010.00185.x. [PubMed: 21392318]

[6]. Wu X, Franka R, Svoboda P, Pohl J, Rupprecht CE, Development of combined vaccines for rabies and immunocontraception, Vaccine. 27 (2009) 7202–7209. 10.1016/j.vaccine.2009.09.025. [PubMed: 19925954]

[7]. Bansal A, Wu X, Olson V, D’Souza MJ, Characterization of rabies pDNA nanoparticulate vaccine in poloxamer 407 gel, Int. J. Pharm 545 (2018) 318–328. 10.1016/j.ijpharm.2018.05.018. [PubMed: 29746999]

[8]. Bansal A, Gamal W, Wu X, Yang Y, Olson V, D’Souza MJ, Evaluation of an adjuvanted hydrogel-based pDNA nanoparticulate vaccine for rabies prevention and immunocontraception, Nanomedicine Nanotechnol. Biol. Med 21 (2019) 102049. 10.1016/j.nano.2019.102049.

[9]. Scheerlinck J-PY, Greenwood DLV, Particulate delivery systems for animal vaccines, Methods San Diego Calif. 40 (2006) 118–124. 10.1016/j.ymeth.2006.05.023. [PubMed: 16997719]

[10]. Roukens AH, Vossen AC, Bredenbeek PJ, van Dissel JT, Visser LG, Intradermally Administered Yellow Fever Vaccine at Reduced Dose Induces a Protective Immune Response: A Randomized Controlled Non-Inferiority Trial, PLoS ONE. 3 (2008). 10.1371/journal.pone.0001993.

[11]. Machado Y, Duinkerken S, Hoepflinger V, Mayr M, Korotchenko E, Kurtaj A, Pablos I, Steiner M, Stoecklinger A, Lübbers J, Schmid M, Ritter U, Scheiblhofer S, Ablinger M, Wally V, Hochmann S, Raninger AM, Strunk D, van Kooyk Y, Thalhamer J, Weiss R, Synergistic effects of dendritic cell targeting and laser-microporation on enhancing epicutaneous skin vaccination efficacy, J. Control. Release Off. J. Control. Release Soc 266 (2017) 87–99. 10.1016/j.jconrel.2017.09.020.

[12]. WHO. Report of a WHO consultation on intradermal application of humanrabies vaccines, Geneva, Switzerland; 1995., (n.d.).

[13]. Moon S, Wang Y, Edens C, Gentsch JR, Prausnitz MR, Jiang B, Dose sparing and enhanced immunogenicity of inactivated rotavirus vaccine administered by skin vaccination using a microneedle patch, Vaccine. 31 (2013) 3396–3402. 10.1016/j.vaccine.2012.11.027. [PubMed: 23174199]

[14]. von Moos S, Johansen P, Tay F, Graf N, Kündig TM, Senti G, Comparing safety of abrasion and tape-stripping as skin preparation in allergen-specific epicutaneous immunotherapy, J. Allergy Clin. Immunol 134 (2014) 965–967.e4. 10.1016/j.jaci.2014.07.037. [PubMed: 25282570]

[15]. Arya JM, Dewitt K, Scott-Garrard M, Chiang Y-W, Prausnitz MR, Rabies vaccination in dogs using a dissolving microneedle patch, J. Controlled Release. 239 (2016) 19–26. 10.1016/j.jconrel.2016.08.012.

[16]. Scheiblhofer S, Strobl A, Hoepflinger V, Thalhamer T, Steiner M, Thalhamer J, Weiss R, Skin vaccination via fractional infrared laser ablation - Optimization of laser-parameters and adjuvantation, Vaccine. 35 (2017) 1802–1809. 10.1016/j.vaccine.2016.11.105. [PubMed: 28117172]

[17]. Weiss R, Hessenberger M, Kitzmüller S, Bach D, Weinberger EE, Krautgartner WD, Hauser-Kronberger C, Malissen B, Boehler C, Kalia YN, Thalhamer J, Scheiblhofer S, Transcutaneous vaccination via laser microporation, J. Controlled Release 162 (2012) 391–399. 10.1016/j.jconrel.2012.06.031.

[18]. Taetz S, Nafee N, Beisner J, Piotrowska K, Baldes C, Mürdter TE, Huwer H, Schneider M, Schaefer UF, Klotz U, Lehr C-M, The influence of chitosan content in cationic chitosan/PLGA nanoparticles on the delivery efficiency of antisense 2'-O-methyl-RNA directed against telomerase in lung cancer cells, Eur. J. Pharm. Biopharm. Off. J. Arbeitsgemeinschaft Pharm. Verfahrenstechnik EV. 72 (2009) 358–369. 10.1016/j.ejpb.2008.07.011.

[19]. Bansal A, Kapoor DN, Kapil R, Chhabra N, Dhawan S, Design and development of paclitaxel-loaded bovine serum albumin nanoparticles for brain targeting, Acta Pharm. Zagreb Croat. 61 (2011) 141–156. 10.2478/v10007-011-0012-8.

[20]. Kasturi SP, Sachaphibulkij K, Roy K, Covalent conjugation of polyethyleneimine on biodegradable microparticles for delivery of plasmid DNA vaccines, Biomaterials. 26 (2005) 6375–6385. 10.1016/j.biomaterials.2005.03.043. [PubMed: 15913771]

[21]. Pai Kasturi S, Qin H, Thomson KS, El-Bereir S, Cha S, Neelapu S, Kwak LW, Roy K, Prophylactic anti-tumor effects in a B cell lymphoma model with DNA vaccines delivered on polyethylenimine (PEI) functionalized PLGA microparticles, J. Controlled Release. 113 (2006) 261–270. 10.1016/j.jconrel.2006.04.006.

[22]. Bordelon H, Biris AS, Sabliov CM, Todd Monroe W, Characterization of Plasmid DNA Location within Chitosan/PLGA/pDNA Nanoparticle Complexes Designed for Gene Delivery, J. Nanomater. 2011 (2010) e952060. 10.1155/2011/952060.

[23]. Ganti SS, Banga AK, Non-Ablative Fractional Laser to Facilitate Transdermal Delivery, J. Pharm. Sci. 105 (2016) 3324–3332. 10.1016/j.xphs.2016.07.023. [PubMed: 27624669]

[24]. Khan MAH, Ferro VA, Koyama S, Kinugasa Y, Song M, Ogita K, Tsutsui T, Murata Y, Kimura T, Immunisation of male mice with a plasmid DNA vaccine encoding gonadotrophin releasing hormone (GnRH-I) and T-helper epitopes suppresses fertility in vivo, Vaccine. 25 (2007) 3544–3553. 10.1016/j.vaccine.2007.01.089. [PubMed: 17316929]

[25]. Pedersen GK, Höschler K, Øie Solbak SM, Bredholt G, Pathirana RD, Afsar A, Breakwell L, Nøstbakken JK, Raae AJ, Brokstad KA, Sjursen H, Zambon M, Cox RJ, Serum IgG titres, but not avidity, correlates with neutralizing antibody response after H5N1 vaccination, Vaccine. 32 (2014) 4550–4557. 10.1016/j.vaccine.2014.06.009. [PubMed: 24950357]

[26]. Jinshu X, Jingjing L, Duan P, Zheng Z, Ding M, Jie W, Rongyue C, Zhuoyi H, Roque RS, A synthetic gonadotropin-releasing hormone (GnRH) vaccine for control of fertility and hormone dependent diseases without any adjuvant, Vaccine. 23 (2005) 4834–4843. 10.1016/j.vaccine.2005.05.010. [PubMed: 15996796]

[27]. Tawde SA, Chablani L, Akalkotkar A, D'Souza C, Chiriva-Internati M, Selvaraj P, D'Souza MJ, Formulation and evaluation of oral microparticulate ovarian cancer vaccines, Vaccine. 30 (2012) 5675–5681. 10.1016/j.vaccine.2012.05.073. [PubMed: 22750042]

[28]. Bansal A, D'Sa S, D'Souza MJ, Biofabrication of microcapsules encapsulating beta-TC-6 cells via scalable device and in-vivo evaluation in type 1 diabetic mice, Int. J. Pharm. 572 (2019) 118830. 10.1016/j.ijpharm.2019.118830. [PubMed: 31715349]

[29]. Caraher EM, Parenteau M, Gruber H, Scott FW, Flow cytometric analysis of intracellular IFN-gamma, IL-4 and IL-10 in CD3(+)4(+) T-cells from rat spleen, J. Immunol. Methods. 244 (2000) 29–40. [PubMed: 11033016]

[30]. Pala P, Hussell T, Openshaw PJ, Flow cytometric measurement of intracellular cytokines, J. Immunol. Methods. 243 (2000) 107–124. [PubMed: 10986410]

[31]. Kapadia CH, Tian S, Perry JL, Sailer D, Christopher Luft J, DeSimone JM, Extending antigen release from particulate vaccines results in enhanced antitumor immune response, J. Control. Release Off. J. Control. Release Soc. 269 (2018) 393–404. 10.1016/j.jconrel.2017.11.020.

[32]. Alam MM, Arifuzzaman M, Ahmad SM, Hosen MI, Rahman MA, Rashu R, Sheikh A, Ryan ET, Calderwood SB, Qadri F, Study of avidity of antigen-specific antibody as a means of understanding development of long-term immunological memory after Vibrio cholerae O1 infection, Clin. Vaccine Immunol. CVI. 20 (2013) 17–23. 10.1128/CVI.00521-12. [PubMed: 23114701]

[33]. Gongal G, Sampath G, Introduction of intradermal rabies vaccination - A paradigm shift in improving post-exposure prophylaxis in Asia, Vaccine. 37 Suppl 1 (2019) A94–A98. 10.1016/j.vaccine.2018.08.034. [PubMed: 30150166]

[34]. Foged C, Hansen J, Agger EM, License to kill: Formulation requirements for optimal priming of CD8+ CTL responses with particulate vaccine delivery systems, Eur. J. Pharm. Sci. 45 (2012) 482–491. 10.1016/j.ejps.2011.08.016.

[35]. Cribbs DH, Ghochikyan A, Vasilevko V, Tran M, Petrushina I, Sadzikava N, Babikyan D, Kesslak P, Kieber-Emmons T, Cotman CW, Agadjanyan MG, Adjuvant-dependent modulation of Th1 and Th2 responses to immunization with β-amyloid, Int. Immunol. 15 (2003) 505–514. 10.1093/intimm/dxg049. [PubMed: 12663680]

[36]. Siel D, Loaiza A, Vidal S, Caruffo M, Paredes R, Ramirez G, Lapierre L, Briceño C, Pérez O, Sáenz L, The immune profile induced is crucial to determine the effects of immunocastration over gonadal function, fertility, and GnRH-I expression, Am. J. Reprod. Immunol. N. Y. N 1989. 79 (2018). 10.1111/aji.12772.

[37]. Hessenberger M, Weiss R, Weinberger EE, Boehler C, Thalhamer J, Scheiblhofer S, Transcutaneous delivery of CpG-adjuvanted allergen via laser-generated micropores, Vaccine. 31 (2013) 3427–3434. 10.1016/j.vaccine.2012.09.086. [PubMed: 23273971]

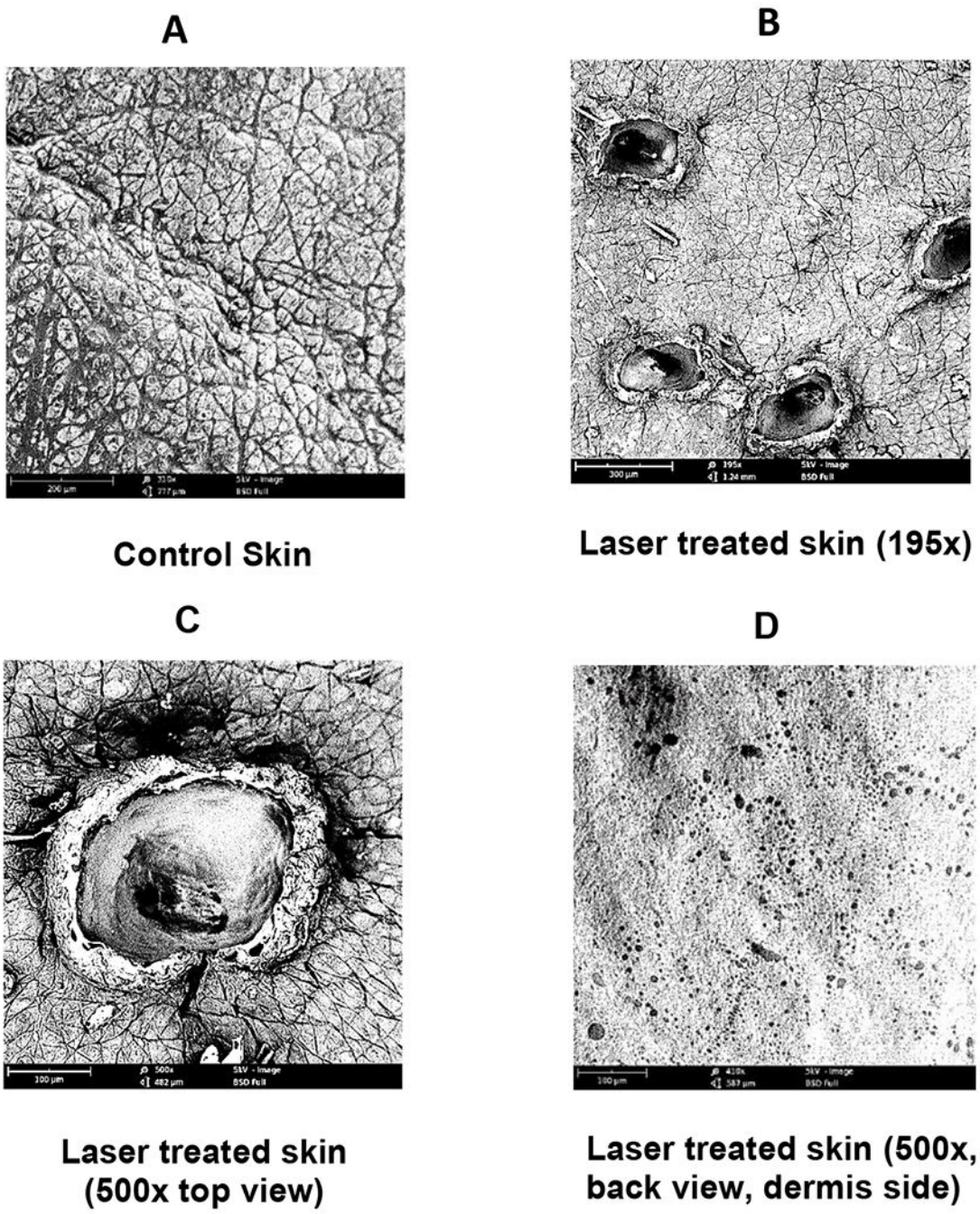

Figure 1 –.

Scanning electron microscopic images (SEM) of laser-treated mice (Swiss Webster) skin. SEM images of (a) control skin sample (Top view, 310×), (b) laser treated skin sample (top view, 195×), (c) laser treated skin sample (top view, 500×), (d) laser treated skin sample (back view i.e. dermis side, 500×).

Figure 2 –.

Image of shaved mouse treated with laser using parameters i.e. pulse 2, pore array 8 mm, and density (7%). Images of laser treated mice skin were taken daily till day 8. Complete skin recovery was observed on day 8, however, the recovery process started on day 3 characterized by

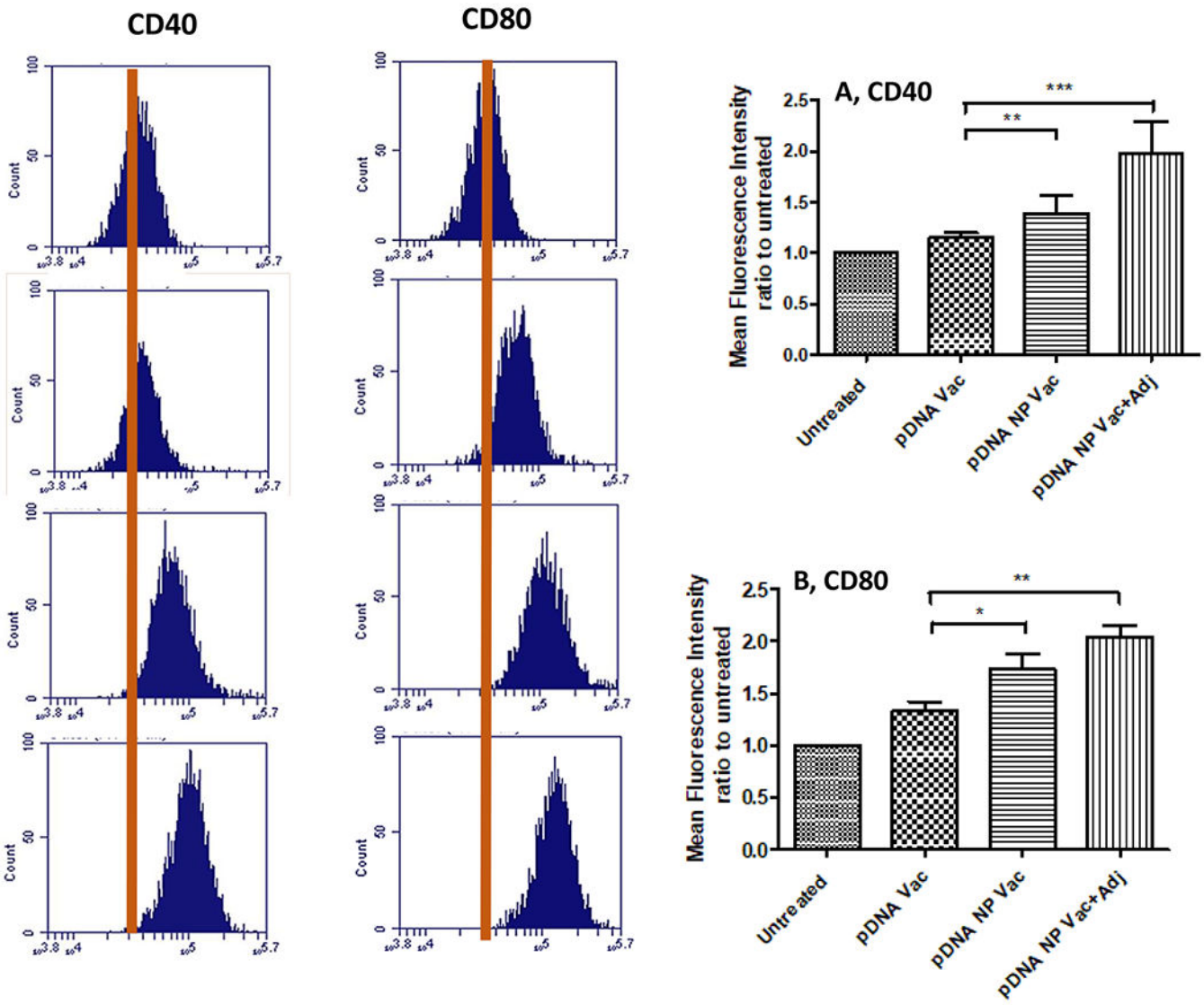

Figure 3 –.

Upregulation of maturation markers i.e. CD40 and CD80 on DC 2.4 post-exposure to various treatment groups. The expression of co-stimulatory molecules was detected by flow cytometry analysis of fluorescence labelled CD80 and CD40 antibodies. Mean fluorescence intensity (MFI) ratios of treatment samples were plotted to untreated samples. Results were analyzed using one way ANOVA followed by post hoc Tukey's multiple comparison test (*$p < 0.05$ significant, **$p < 0.01$ very significant, ***$p < 0.001$ extremely significant). Data are expressed as mean ± SEM, n=3.

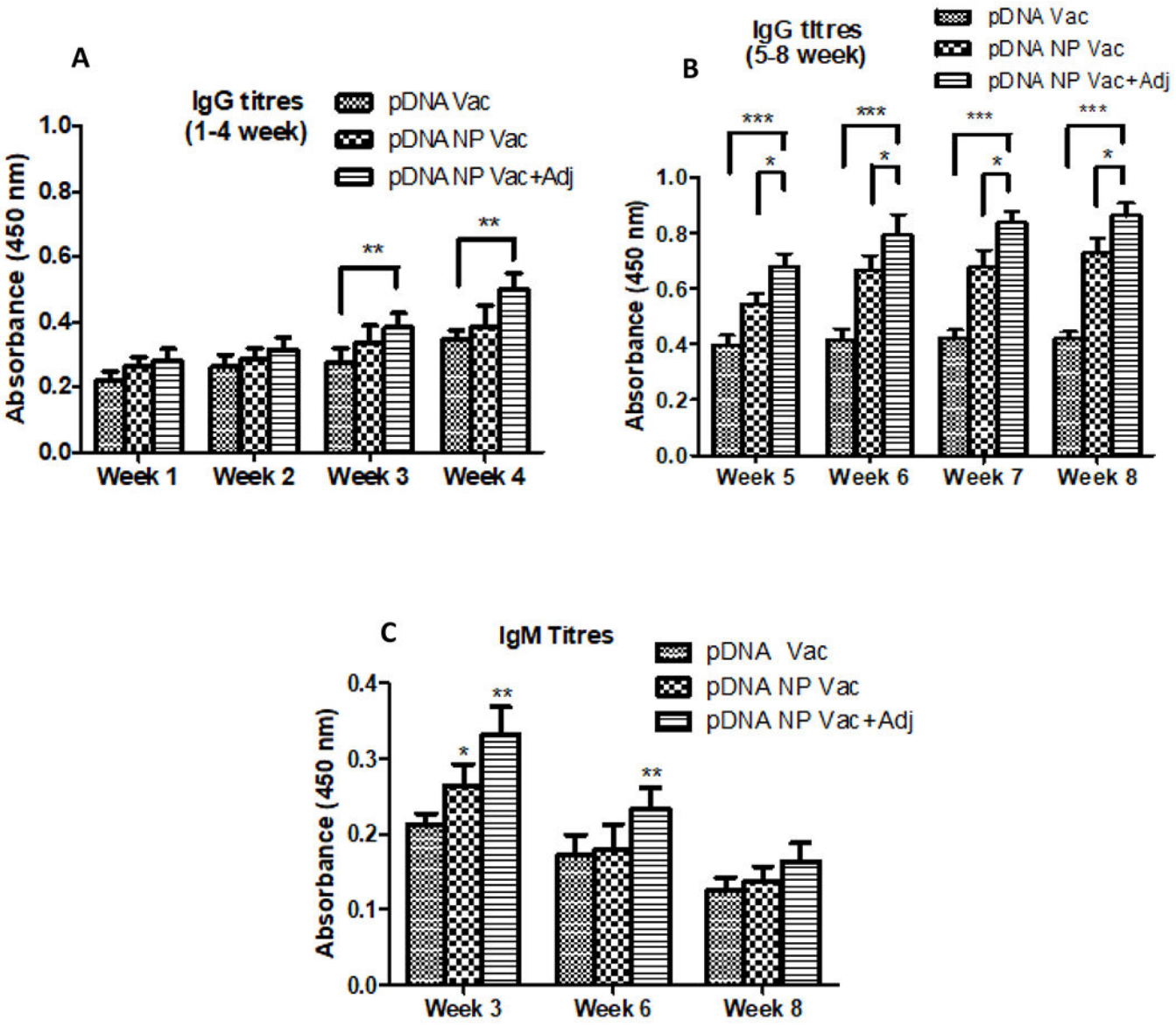

Figure 4 –.

Serum antibody titers (IgG and IgM) in mice after vaccination with rabies vaccines via intradermal route. Mice (n=6) were vaccinated on day 1 with, pDNA (25 μg) in hydrogel, pDNA nanoparticulate vaccine and pDNA nanoparticulate vaccine plus adjuvant in hydrogel. Blood was collected every week post vaccination and analyzed for anti-GnRH antibodies using ELISA. Results were compared statistically among groups every week (*$p < 0.05$ significant, **$p < 0.01$very significant, ***$p < 0.001$ extremely significant) using one-way ANOVA with Tukey post hoc test. Data are expressed as mean ± SEM.

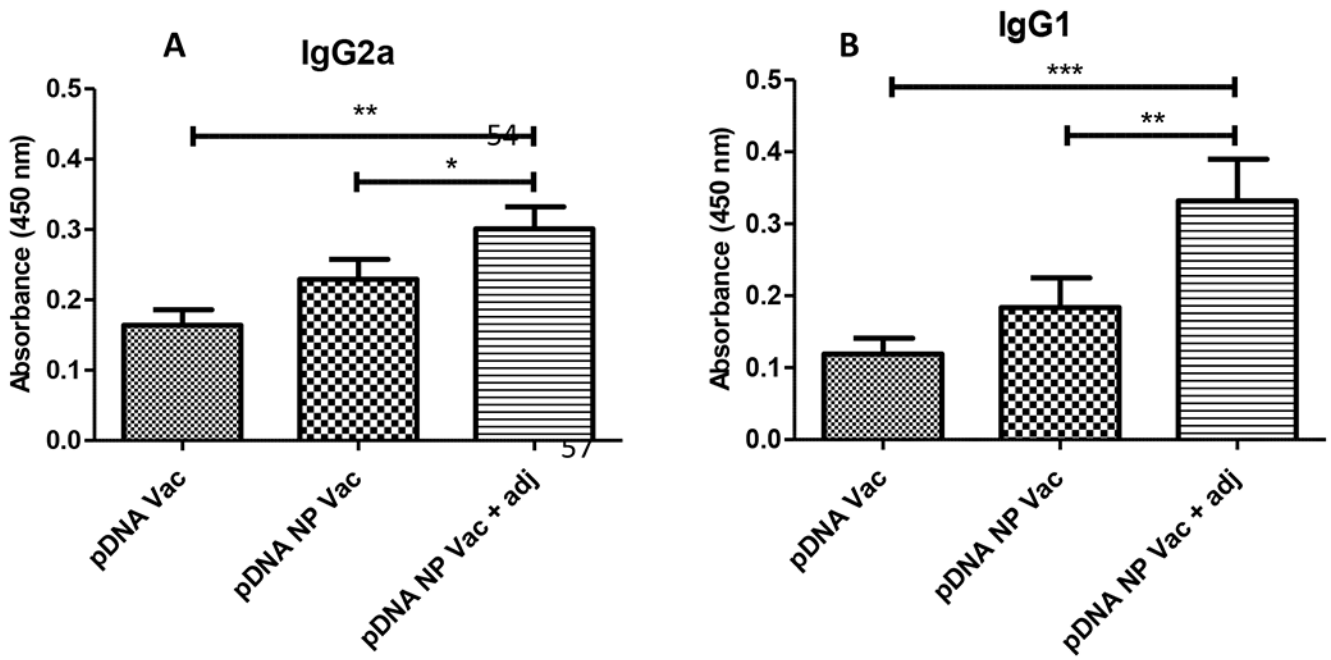

Figure 5 –.

The anti-GnRH specific IgG subclass immune response. IgG subclass (IgG1, IgG2a) titers were measured in sera of mice (n=6) post vaccination collected on week 6. *p* value was calculated (*p < 0.05 significant, **p < 0.01very significant, ***p < 0.001 extremely significant) using one-way ANOVA with Tukey post hoc test. Data are expressed as mean ± SEM.

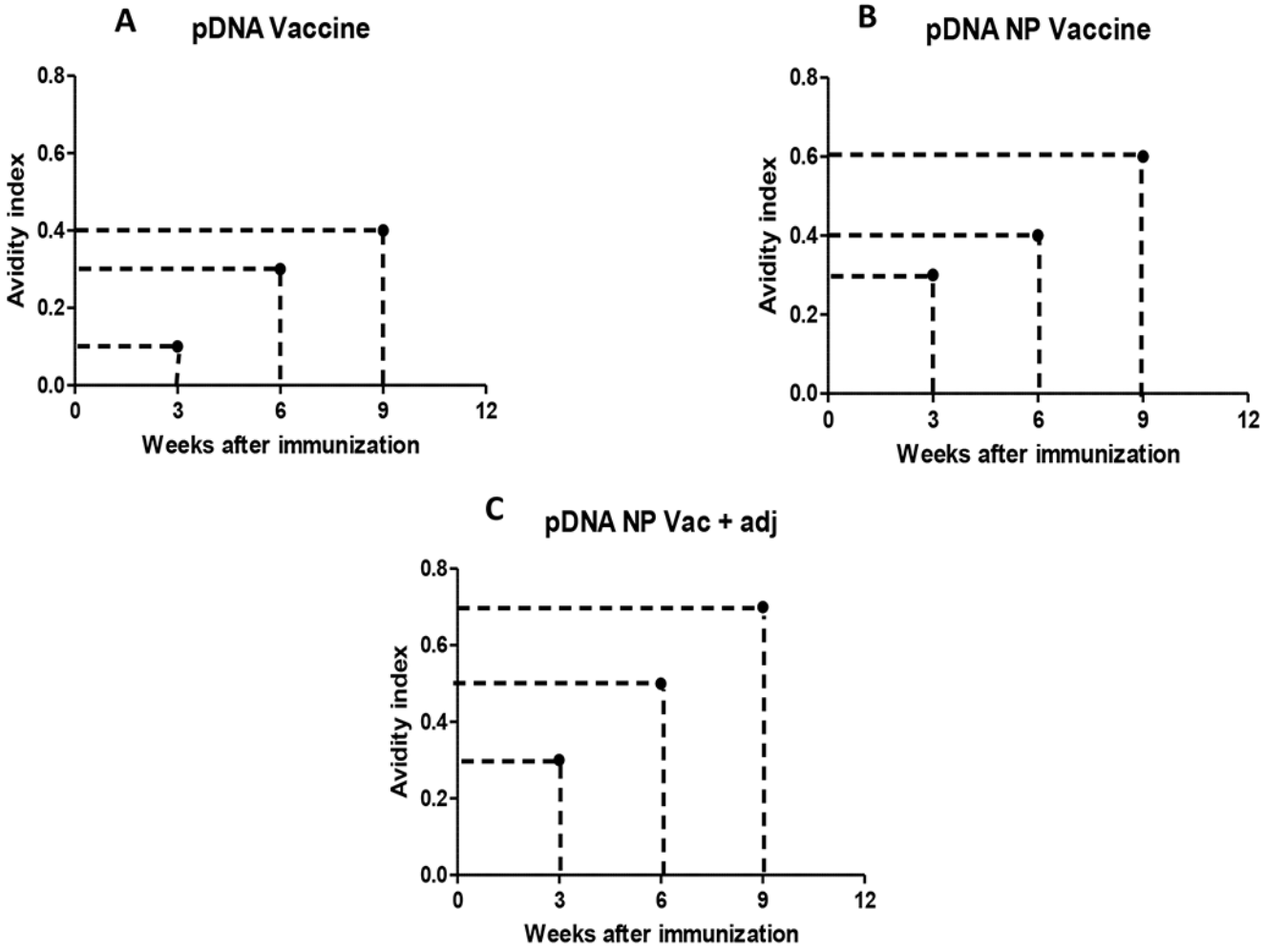

Figure 6 –.

Avidity index was determined by incubating serum with increasing concentrations of sodium thiocyanate and calculated as 50% reduction in absorbance from untreated samples. The three groups used for the study were, pDNA vaccine, pDNA nanoparticulate vaccine and pDNA nanoparticulate vaccine plus adjuvants (alum and MF59) and samples were measured for AI at weeks 3, 6 and 9.

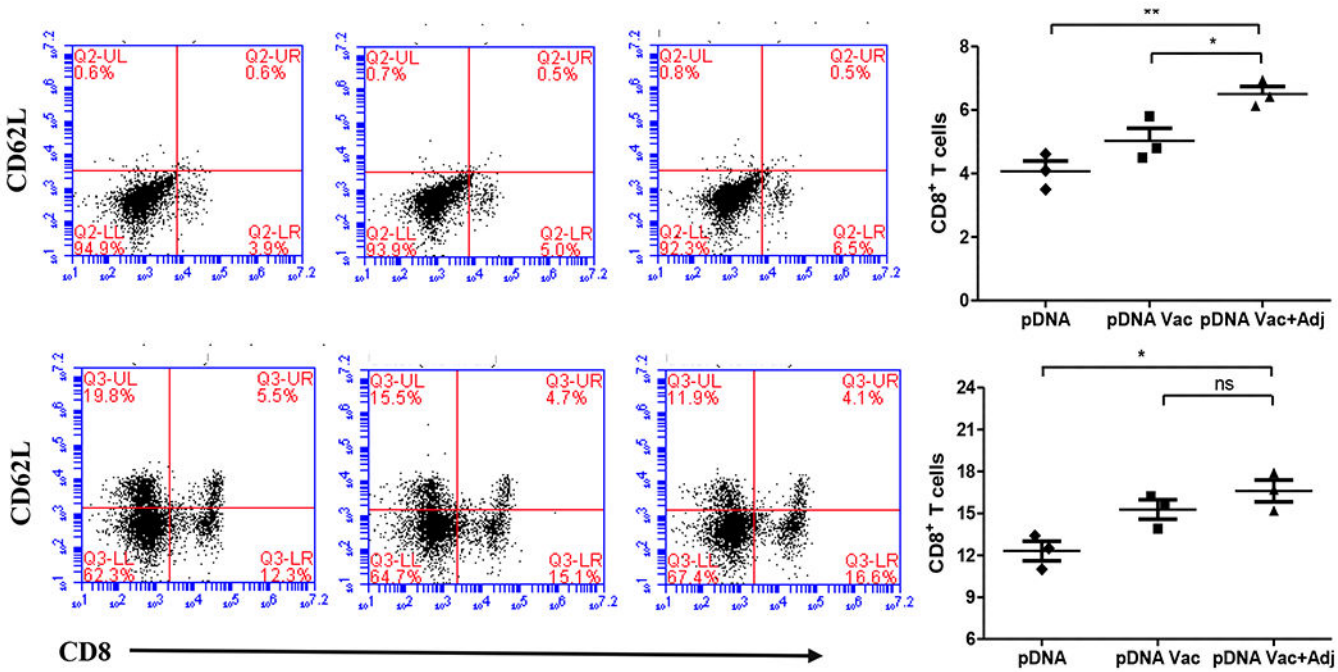

Figure 7 -

The percentage of $CD8^+$ and CD62L positive cells in both splenocytes (top) and lymph node cells (bottom) were evaluated after re-stimulation with antigen. Representative flow cytometry dot plots for each group are shown. Plots shown in Figure 7A & 7B showed the CD8 positive cells in splenocytes and lymphnode cells. *p* value was calculated (*p < 0.05 significant, **p < 0.01 very significant, ***p < 0.001 extremely significant) using one-way Anova, multiple comparison was performed using tukey's post hoc analysis. Data are expressed as mean ± SEM.

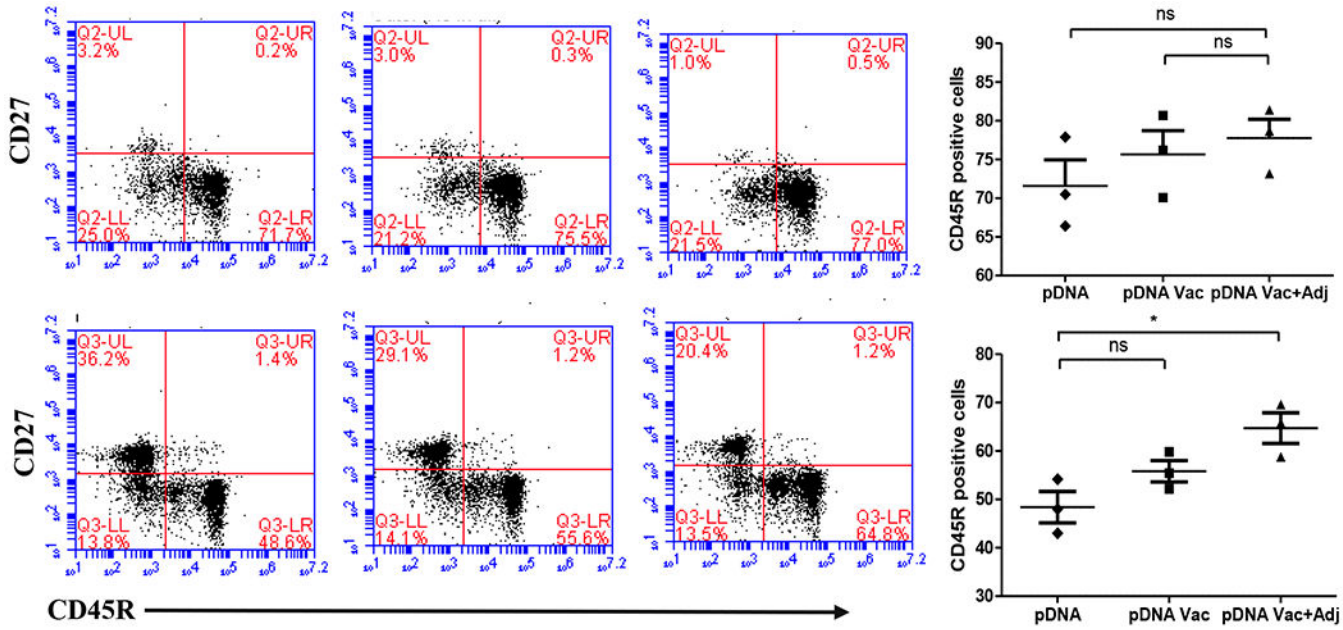

Figure 8 -

The percentage of CD45R and CD27 positive cells in both splenocytes (top) and lymph node cells (bottom) were evaluated after re-stimulation with antigen. Representative flow cytometry dot plots for each group are shown. Plots in Figure 8A & 8B showed the CD45R positive cells in splenocytes and lymphnode cells. *p* value was calculated (*p < 0.05 significant, **p < 0.01 very significant, ***p < 0.001 extremely significant) using one-way Anova, multiple comparison was performed using tukey's post hoc analysis. Data are expressed as mean ± SEM.

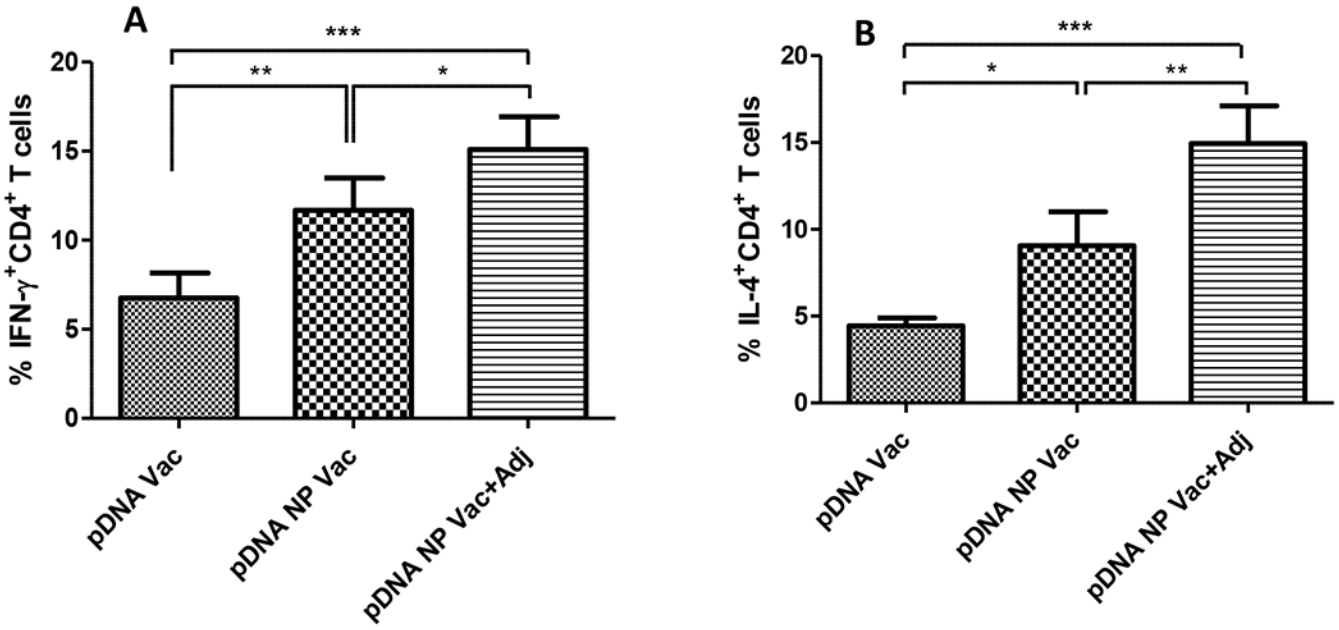

Figure 9 –.

Induction of IFN-γ and IL-4 cytokine expression by $CD4^+$ T cells. Increased expression of IFN-γ cytokine results in Th1 mediated cytotoxic immune response and IL-4 cytokine expression dictates Th2 mediated humoral immune response. The cytokines expression were determined by intracellular staining of mice splenocytes with IL-4 and IFN-γ antibodies and analyzed via flow cytometry. Results were analyzed using one way ANOVA followed by post hoc Tukey's multiple comparison test (*$p < 0.05$ significant, **$p < 0.01$ very significant, ***$p < 0.001$ extremely significant). Data are expressed as mean ± SEM, n=3.